8 (3): 198-205 (2024)

Journal of Aviation

https://dergipark.org.tr/en/pub/jav

e-ISSN 2587-1676

# Design and Implementation of A Low-Cost Parachute Landing System for Fixed-Wing Mini Unmanned Aerial Vehicles

**Fatma Yıldırım Dalkıran[1*], Emre Kırteke[2,3]**

[1*] Erciyes University, Faculty of Aeronautics and Astronautics, Kayseri, Türkiye. (fatmay@erciyes.edu.tr)
[2] Kapadokya University, Aircraft Technology, Nevşehir, Türkiye. (emre.kirteke@kapadokya.edu.tr)
[3] Erciyes University, Graduate School of Natural and Applied Sciences, Kayseri, Türkiye.

Article Info

Received: 06 May 2024
Revised: 26 August 2024
Accepted: 23 September 2024
Published Online: 06 October 2024

Keywords:
Fixed UAV
Parachute
Parachute Landing System
Parachute Fabric

Corresponding Author: *Fatma Yıldırım Dalkıran*

RESEARCH ARTICLE

https://doi.org/10.30518/jav.1479457

## Abstract

Fixed-wing mini-UAVs (Unmanned Aerial Vehicles) face difficulties due to the need for runways during take-off and landing. While fixed-wing UAVs are capable of using catapults during take-off, various landing systems are required for landing. Therefore, in this study, a parachute system design and production were carried out for the safe landing of fixed-wing mini-UAVs. The produced parachute utilized ultra-lightweight ripstop nylon fabric and suspension lines, while a carbon fiber tube was chosen for the launching system for its lightweight and strength. The parachute deployment system was triggered by a servo motor with low power consumption and high torque. During tests, the parachute was activated at a height of 47 meters during flight. The parachute deployment was completed in 1.42 seconds, and the descent with the parachute lasted 11 seconds. The vertical descent speed of the parachute during landing was measured at 4.27 m/s. The produced parachute landing system was manufactured at 71% lower cost compared to existing parachute landing systems in the literature and on the market. Additionally, the ultra-light ripstop parachute weighed 56 grams, making it 12% lighter than similar systems. Considering the advantages in terms of cost and weight, it is anticipated that parachute landing systems will be increasingly used for fixed-wing UAVs in the future.

## 1. Introduction

**U**nmanned **A**erial **V**ehicles (UAVs) have seen a significant expansion in their utilization in recent years due to advancements in technology. While UAVs are classified into fixed-wing, rotary-wing, and hybrid types, they can also be categorized based on their size, mission system, and weight. UAVs weighing less than 20 kg are referred to as mini-UAVs. Controlling and ensuring the flight stability of mini-UAVs, which have smaller dimensions and lower weight, pose greater challenges. Various measures have been initiated to ensure flight safety (Austin, 2010).

It is well known that UAVs have higher accident rates compared to manned aircraft. Many UAV accidents related to human factors occur during take-off and landing. Landing is one of the most challenging tasks for pilots. Proper guidance towards the landing area and maintaining an appropriate approach angle are essential for aircraft. Statistics provided by Boeing indicate that 53% of fatal accidents occur during landing or take-off phases. Efforts are underway to reduce these accident rates in UAVs, with particular emphasis on ensuring safe landings (Kim et al., 2013; Oktay et al., 2016; Williams, 2004).

Bellis investigated the design and production steps of parachute landing systems for fixed-wing UAVs. The research revealed that the rescue system should be safe, reliable, and predictable (Bellis, 2019; Wilson, 2024). Furthermore, some techniques have been developed to allow continuous use of parachute rescue systems. Determining the types of parachutes is crucial due to their variable drag coefficient values. Among these types, the most commonly used ones are the dome, cruciform and parafoil structures. It is anticipated that dome and cruciform structures will be more suitable for current UAVs, while parafoil systems are considered to be open to development and expected to be used more in the future (Wyllie, 2001).

In literature another study was related with a parachute landing system to rescue and assist in the landing of fixed-wing mini-UAVs (Zakaria, 2013). He anticipated the use of three different parachute canopies for the parachute landing system. He calculated that using a parachute canopy with a parafoil structure would not be efficient, as this type of parachute would drag the UAV. He stated that the cruciform parachute canopy is the simplest design and could be easily manufactured, but it has a low drag coefficient and is not suitable for flight safety. Therefore, due to its high drag coefficient, reliability, and non-steerable parachute type, he used the round parachute canopy in his study.

(Gleason and Fahlstrom, 2016) discussed seven different UAV recovery systems. The first one is conventional landing, where a landing gear and wheels are added to the UAV for runway landing. They mentioned that a net system could be used for this purpose, but it could potentially damage the UAV during recovery. In this study in the parachute recovery

system, it was emphasized that a parachute with a parafoil structure should be preferred due to its high stability and low landing speed in this study. VTOL (Vertical Take-off and Landing) UAVs were considered to have vertical take-off and landing capabilities, making this feature valuable as a landing system. Regarding air recovery systems, it was suggested that while the UAV is airborne with a parachute deployed, it could be hooked up by another aircraft for mid-air recovery. Ship recovery systems were also discussed, highlighting the need to design the recovery system considering certain ship-related issues (Gleason and Fahlstrom, 2016).

In the study conducted by (Abinaya and Arravind, 2017), the low-cost design of UAV recovery and landing systems was investigated. Traditional wheeled landing, skid landing, net recovery, parachute recovery, and mid-altitude recovery methods were examined in this study, discussing their advantages and disadvantages. Additionally, each recovery method was compared with others in terms of parameters such as cost, safety, operator requirements, complexity, and success rate in recovery (Abinaya and Arravind, 2017).

In UAV parachute recovery systems, externally produced and subsequently added payloads are available. Companies such as Fruity Chutes, Tulpar Space Aviation and Defense Co., Mars Parachutes, Butler Company, and My Research Company commercially manufacture and sell parachute systems (Ultimate Drone Parachute System for All Multicopters, Fixed Wing, UAS, 2024). Fruity Chutes indicated that for rotary-wing UAVs, a spring system and $CO_2$-based ballistic launchers could be utilized. For fixed-wing UAVs, the use of a pilot chute was recommended to allow the parachute to meet free air. Additionally, they offer various parachute options to ensure the selection of the most suitable parachute for the UAV.

## 2. Parachute Landing System Design for Fixed-Wing Mini UAVs

With the increasing utilization of fixed-wing mini-UAVs for observation and reconnaissance purposes in civilian areas, the need for these UAVs to be capable of taking off and landing near residential areas has arisen (Blom, 2010). However, while UAVs can utilize a catapult for take-off, they still require a runway for landing. To eliminate the need for a runway, this study focuses on the design and production of a parachute landing system for mini-UAVs. Parachutes are devices that utilize basic physics and aerodynamic equations to slow down the descent speed of objects and provide stability by harnessing frictional forces. With a rich history, parachutes have diverse applications, and are commonly used in aviation practices today. Parachute systems are widely used for UAVs as emergency recovery systems and for landings in confined spaces. The design of a parachute and launch mechanism for the safe landing of fixed-wing mini-UAVs has been developed in this study. In this design, the total weight of the UAV was first calculated, and accordingly, calculations for the required parachute area and parachute diameter were made. The first step in parachute system design is to determine the type of parachute. Parachute types vary depending on parameters such as drag coefficient, opening force, and average swing angle (Knacke, 1991). Parachute types can be categorized into three main types: round, cruciform, and parafoil (ram-air). Among these, round parachutes have the highest drag coefficient, but their high swing angle may cause damage when used with UAVs (Historical Review, 2024). Cruciform parachute types have a low swing angle but are not preferred due to their lower drag coefficient compared to round parachutes (Different parachute types: Styles of canopy for skydiving, 2024). Parafoil parachutes have a very high drag coefficient, but their high glide ratio makes them very difficult to use in residential areas (Szafran and Kramarski, 2019). However, advancements in round parachutes have led to the emergence of annular, or pull-down apex, and conical parachutes. The purpose of these developments in round parachutes is to reduce the average swing angle and increase stability. Therefore, an annular type parachute is used in our parachute system. (Kekeç et al., 2020; Parachute, 2024).

Alongside the parachute type, one of the paramount considerations is the selection of parachute system components. These encompass the parachute fabric, parachute cord, and connecting elements. Optimal choices for the parachute canopy entail durable, elastic, and tear-resistant nylon fabrics. Known as ripstop, tear-resistant nylon fabric is woven using a specialized technique during fabrication. In ripstop fabrics, a grid pattern is formed by weaving threads in perpendicular directions, thereby fostering a robust fabric structure. This methodology aims to impede thread displacement and enhance fabric resilience, preventing the propagation of minor tears. Hence, our parachute design incorporates ultra-lightweight ripstop nylon fabric for both the canopy and suspension cord (Federal Aviation Administration, 2015; Poynter, 1991).

In parachute design, the initial step involves calculating the total mass and determining the desired drag coefficient to be produced by the parachute. Such variables as parachute configuration and surface area can be readily computed based on the specified drag coefficient. The linkage between the total weight exerted on the parachute and the resultant drag force generated by the parachute is delineated by Equation (1).

$$F_D = mg \tag{1}$$

Equation (1) represents $F_D$ as the drag force, m as the mass, and g as the gravitational acceleration. Equation (2) depicts the drag force.

$$F_D = \frac{1}{2}\rho V_p^2 C_D S_p \tag{2}$$

$C_D$ represents the drag coefficient, $S_p$ is the projected area of the parachute, $V_P$ is the parachute velocity, and $\rho$ is the air density. Equation (3) is derived from Equations (1) and (2).

$$\frac{1}{2}\rho V_p^2 C_D S_p = mg \tag{3}$$

Once parameters such as mass, parachute descent speed, and drag coefficient are determined, the required surface area for the parachute can be calculated as shown in Equation (4).

$$S_p = \frac{2mg}{\rho V_p^2 C_D} \tag{4}$$

Based on the parachute area calculated in Equation (4), the parachute diameter $R_p$ can be calculated according to Equation (5).

$$R_p = 2\sqrt{\frac{S_p}{\pi}} \tag{5}$$

One of the important aspects in the mathematical modelling of the parachute is determining the measurements of the suspension lines. Here, Equation (6) can be derived based on Equation (5).

$$L_p = 1{,}1 * (R_p + S_l) \quad (6)$$

According to Equation (6), $L_p$ represents the measurement of the suspension lines, while $S_l$ indicates the seam or cut allowance. The block diagram of the system's production based on the equations is illustrated in Figure 1.

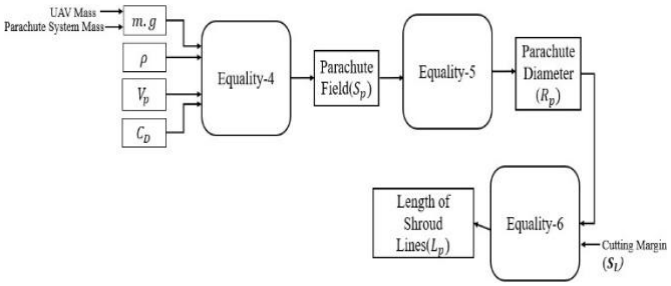


**Figure 1.** Block Diagram of Parachute Design Entry and Exit.

One of the first parameters to be determined when designing parachute systems is the vertical speed of the specified mass. Vertical speed can vary depending on the type of object to be landed. In the case of the UAV system used here, this value is designed to minimize impact energy. By keeping descent speeds high, the parachute diameter and area can be reduced, thereby reducing the total mass of the parachute system. Although parachute designs and types may vary depending on various applications, particular attention should be paid to determining or maintaining vertical speed within certain limits.

It has been observed in the literature that parachute systems can be designed considering different speed values for the landings of UAV systems. One of the fundamental principles here is that designs have been developed according to the UAV payload density. While the landing speed of the parachute system for UAVs varies between 4.5 m/s and 5.5 m/s in the literature (Al-Madani et al., 2018), the parachute system designed in this study is planned to land at a speed of 4.5 m/s.

After determining the parachute diameter, the number of cells and the design of the cells were carried out. Three-dimensional modelling software, or numerical designs, can be used for cell design. In this study, a two-dimensional design process prepared in Excel format was carried out numerically for cell design. The interface and input parameters prepared are shown in Figure 2. The number of cells was determined based on similar studies conducted in the literature and the most preferred systems on the market at a similar scale. In this study, a ten-cell parachute structure was chosen to facilitate production and increase stability.

The Excel file created in Figure 2 provides a practical solution with a simple interface for designing parachute cell layouts that can be produced in different dimensions later on. Here, users can determine the coordinates of the cells to be produced by entering the parachute area and diameter calculated using Equations (4 and 5).

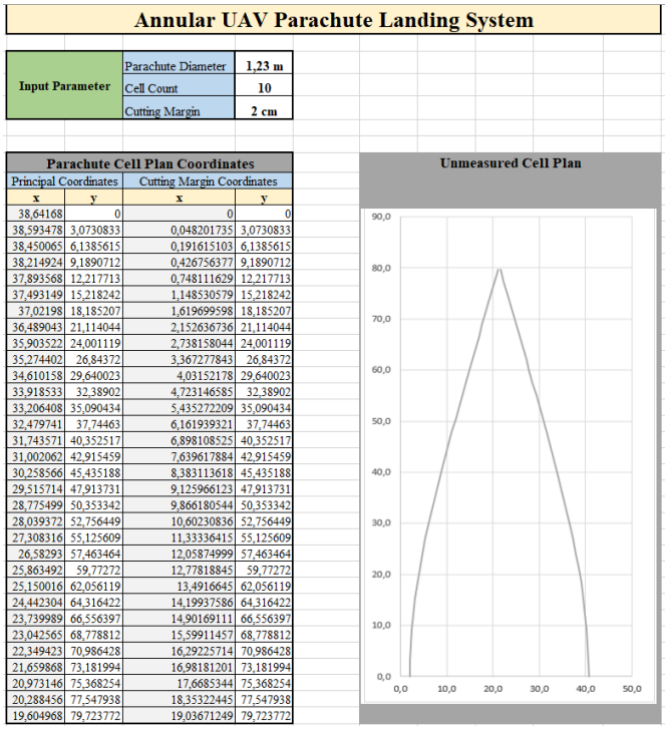

**Annular UAV Parachute Landing System**

| Input Parameter | | |
|---|---|---|
| | Parachute Diameter | 1,23 m |
| | Cell Count | 10 |
| | Cutting Margin | 2 cm |

**Parachute Cell Plan Coordinates**

| Principal Coordinates | | Cutting Margin Coordinates | |
|---|---|---|---|
| x | y | x | y |
| 38,64168 | 0 | 0 | 0 |
| 38,593478 | 3,0730833 | 0,048201735 | 3,0730833 |
| 38,450065 | 6,1385615 | 0,191615103 | 6,1385615 |
| 38,214924 | 9,1890712 | 0,426756377 | 9,1890712 |
| 37,893568 | 12,217713 | 0,748111629 | 12,217713 |
| 37,493149 | 15,218242 | 1,148530579 | 15,218242 |
| 37,02198 | 18,185207 | 1,619699598 | 18,185207 |
| 36,489043 | 21,114044 | 2,152636736 | 21,114044 |
| 35,903522 | 24,001119 | 2,738158044 | 24,001119 |
| 35,274402 | 26,84372 | 3,367277843 | 26,84372 |
| 34,610158 | 29,640023 | 4,03152178 | 29,640023 |
| 33,918533 | 32,38902 | 4,723146585 | 32,38902 |
| 33,206408 | 35,090434 | 5,435272209 | 35,090434 |
| 32,479741 | 37,74463 | 6,161939321 | 37,74463 |
| 31,743571 | 40,352517 | 6,898108525 | 40,352517 |
| 31,002062 | 42,915459 | 7,639617884 | 42,915459 |
| 30,258566 | 45,435188 | 8,383113618 | 45,435188 |
| 29,515714 | 47,913731 | 9,125966123 | 47,913731 |
| 28,775499 | 50,353342 | 9,866180544 | 50,353342 |
| 28,039372 | 52,756449 | 10,60230836 | 52,756449 |
| 27,308316 | 55,125609 | 11,33336415 | 55,125609 |
| 26,58293 | 57,463464 | 12,05874999 | 57,463464 |
| 25,863492 | 59,77272 | 12,77818845 | 59,77272 |
| 25,150016 | 62,056119 | 13,4916645 | 62,056119 |
| 24,442304 | 64,316422 | 14,19937586 | 64,316422 |
| 23,739989 | 66,556397 | 14,90169111 | 66,556397 |
| 23,042565 | 68,778812 | 15,59911457 | 68,778812 |
| 22,349423 | 70,986428 | 16,29225714 | 70,986428 |
| 21,659868 | 73,181994 | 16,98181201 | 73,181994 |
| 20,973146 | 75,368254 | 17,6685344 | 75,368254 |
| 20,288456 | 77,547938 | 18,35322445 | 77,547938 |
| 19,604968 | 79,723772 | 19,03671249 | 79,723772 |



**Figure 2.** 2-Dimensional Parameters of the Produced Parachute.

According to Figure 2, the coordinates on the left side of the table are provided in two different x and y planes. The x and y coordinates on the left side indicate the shape the parachute cell will take after sewing, while the coordinates on the right side indicate the area to be cut from the fabric, including seam allowances. The visual provided on the right shows a preview of the two-dimensional shape created by the coordinates and is not to scale. Figure 3, on the other hand, demonstrates the previously generated cell information from the Excel file scaled and showing their actual dimensions.

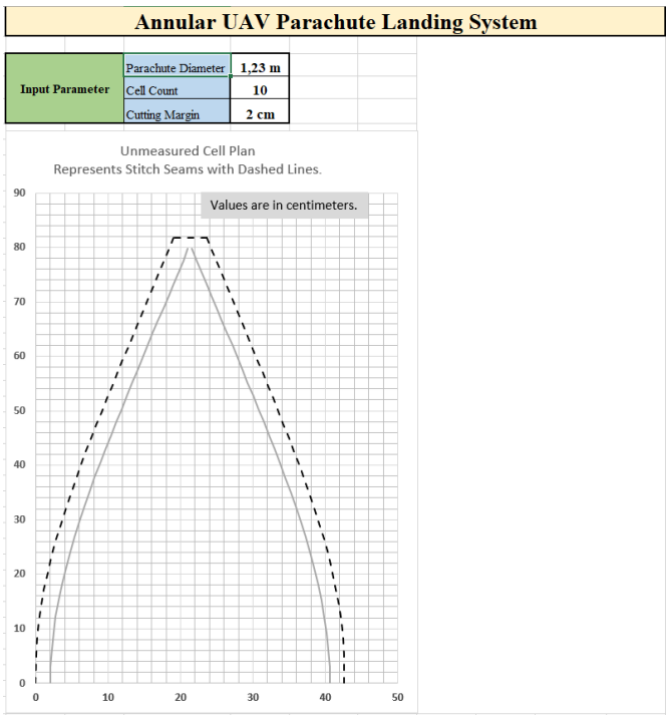

**Annular UAV Parachute Landing System**

| Input Parameter | | |
|---|---|---|
| | Parachute Diameter | 1,23 m |
| | Cell Count | 10 |
| | Cutting Margin | 2 cm |



**Figure 3.** Scaled Parachute Cell Plan.

After placing the cell plans on the fabric and marking them with fabric pens, they were cut. Following the equal and smooth cutting of the ten cells, stitching operations were initiated for their assembly. The quality, frequency, and type of stitching thread are crucial to prevent damage to the cells during their assembly and parachute deployment shock. In this study, TEX 70 model threads were used for stitching, which can withstand high tensile strength values. In this study, utilizing ultra-lightweight fabric technology, TEX 70 threads provide superior durability to eliminate the possibility of abrasion in the stitches. The breaking strength of this thread is specified by the manufacturer as 40 N with a diameter of 0.33 mm. For the assembly of cells, a brother ZE-856/858 industrial sewing machine was used, which allows adjustment of various stitching types and frequencies. Zigzag stitches were specifically used to join the threads with the canopy and apex, enabling the distribution of load on the fabric and threads, especially during instantaneous shock loads. After completing the stitches of the cells, binding was made to prevent fraying and structural disruption of the weft and warp threads in the fabric. Figure 4 illustrates how the folds and seam allowances of the cells are aligned, while Figure 5 demonstrates the joining of two cells, their alignment with zigzag stitches, and the junctions with the load ribbon.

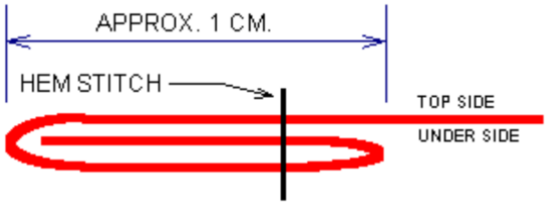


**Figure 4.** Folding and Seam Allowances of Parachute Cells (Nakka, 2020).

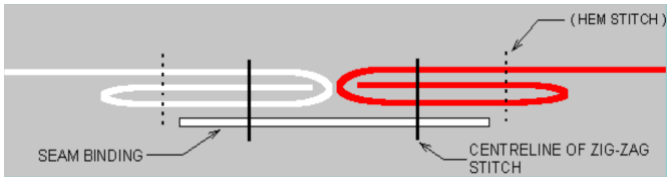


**Figure 5.** Assembly of Parachute Cells and Zigzag Stitching (Nakka, 2020).

One of the critical components of parachute systems is the suspension lines. Proper determination of line dimensions is essential for the safe operation of parachute designs and maintaining consistent drag coefficients. In this study, when calculating line dimensions for the designed and manufactured parachutes, Equation (6) was utilized. The parachute diameter and seam allowance calculated from Equation (5) were applied to Equation (6) to determine the length of line to be used for each cell. For this study, a 2-centimeter seam allowance was set for a 1.23-meters parachute diameter, resulting in line lengths of 1.38 meters. Here, in addition to the parachute line length, an approximately 10-centimeter allowance was left by considering connections to the canopy, seam allowances, and all lines' connection to the UAV for cutting the lines. The suspension lines used for the parachute are characterized by their ripstop and 100% nylon structure, providing natural durability and flexibility. Additionally, it has been noted that the suspension lines exhibit high tensile strength over 100 kg and minimal elongation or shortening during prolonged use. Furthermore, compared to suspension lines used in many parachute landing systems designed for UAVs, these lines have a lower weight.

The release mechanism for parachute systems is crucial for both protecting the parachute and enabling it to open when needed. Therefore, release mechanisms are designed to allow for different designs and release systems, as well as triggering the parachute using servo motors or ballistic systems. Release mechanism body parts are typically made of composite materials, as well as plastics or aluminium alloys. In this study, carbon fiber and PLA parts were used for the release mechanism, chosen for their cost-effectiveness and lightness. The release mechanism, designed using 3D solid modelling software like SolidWorks, consists of 4 different PLA parts and was produced using a 3D printer.

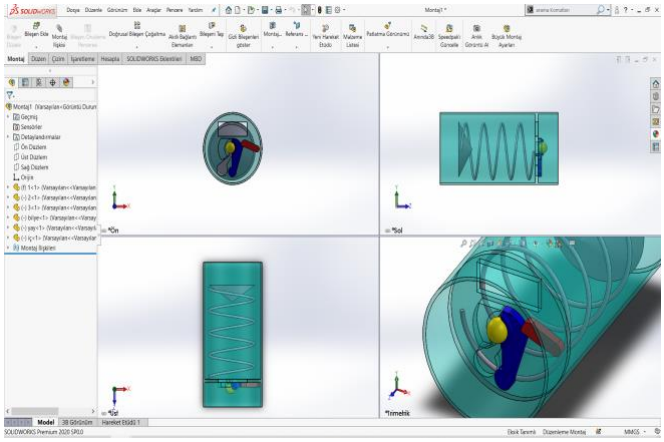

**Figure 6.** Solidworks designs of the parachute deployment mechanism.

During the production stage, parts designed using SolidWorks software were saved in STL format and transferred to CURA software for conversion to Gcode format. In CURA, the density of the parts was set to 50%, and they were adjusted for printing from an Ender3 model printer. The produced parts are shown in Figure 7.

**Figure 7.** Representation of CURA software and produced PLA parts.

The launch mechanism is used to release the parachute upon command from the pilot. For this purpose, the system utilizes the force exerted by a spring to rapidly deploy the parachute without being attached to the aircraft or its subsystems during flight. Prior to flight, the launch mechanism is set up to lock the tension of the spring using a servo motor to prevent its release. Thus, unless commanded by the pilot, the servo motor will store the energy of the spring, preventing the parachute from being launched. Figure 8 illustrates the response of the launch mechanism in its closed and open positions.

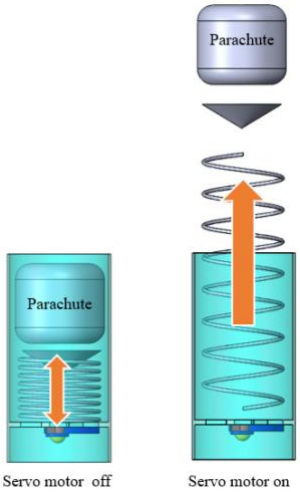


**Figure 8.** Illustration of the open and closed positions of the parachute launch mechanism.

The use of PLA parts and carbon fiber tubes in the launch mechanism has significantly minimized costs. Furthermore, the avoidance of heavy metals commonly found in similar products has resulted in less impact on the UAV take-off weight. This has demonstrated the potential to alleviate problems encountered by users with flight durations in similar systems. Additionally, the stable operation of the launch mechanisms, along with the systematic folding of parachutes and cords within them, is crucial for the system. Hence, the ability for the annular configuration parachute produced to be easily and quickly folded will provide a significant advantage to users.

Ground tests of the parachute launch mechanism have enabled the observation of the system's stability and its response in potential emergency scenarios. Following ground tests, the integration of the UAV and parachute system was performed. The total mass of the parachute landing system was estimated to be 500g during the design phase, but it was measured at 465 g after production. To ensure that the parachute system does not compromise the structural integrity of the UAV, epoxy resin and plywood supports were added to the areas where the launch mechanism was installed.

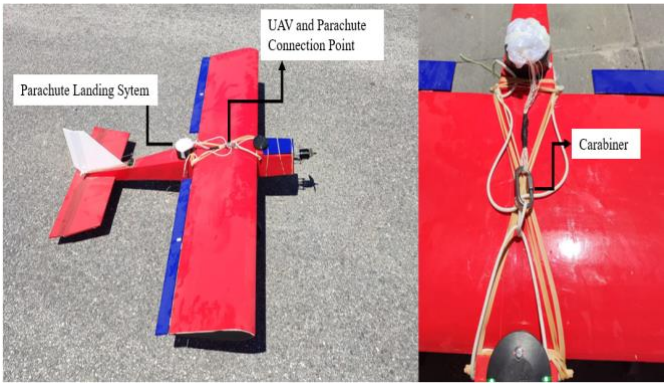


**Figure 9.** Presentation of the Parachute Landing System on the UAV.

After the parachute is deployed, it is essential to establish a connection between the parachute and the UAV for the safe landing of the UAV. This connection point also creates a shock force based on the weight and acceleration of the UAV. To prevent damage to the system and ensure that the parachute does not detach, the UAV parachute connection was made using a 3mm aluminium carabiner. The positioning of the connection near the center of gravity or in close proximity to it is crucial for the safe landing of the UAV. Therefore, in this study, the parachute and UAV connection were positioned very close to the center of gravity. Figure 9 depicts the connection point on the wing where the UAV will be carried by the parachute after deployment.

## 3. Result and Discussion

After the successful completion of ground tests for the UAV electronics and launch mechanism, real flight tests were conducted. For the test flights, the Talas Municipality Model Aircraft Runway located in the Kayseri Talas district, away from residential areas, was chosen. Initially, to ensure flight safety, the calibration of the flight controller and telemetry communication distance were tested in the flight area. After rechecking the UAV's center of gravity, battery levels, and structural components, thrust testing of the brushless motor and trim adjustments of the servo motors were performed. Following the verification of the SW-A switch connection used for parachute triggering, the GPS satellite count and signal quality were also checked. After a short flight of 2 minutes and 36 seconds, the parachute landing system was activated, and a safe landing of the UAV was observed.

Post-flight checks revealed no damage to the UAV's structural components, electronics, or parachute landing system. During the brief flight, the UAV took off under pilot control in stabilize mode and was brought to a balanced flight position with minor trim adjustments after reaching a certain altitude post-take-off. Subsequently, the parachute was deployed using the SW-A switch over a suitable area by the pilot. Upon issuing the triggering command, the parachute fully deployed in 1.42 seconds. Pre-flight, flight, and landing with the parachute are illustrated in Figure 10.

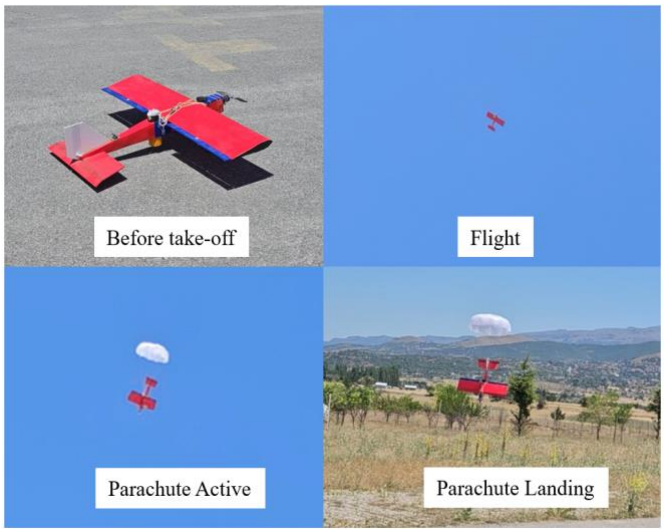


**Figure 10.** Phases of UAV Flight.

During the flight, a total distance of 2.68 km was covered, reaching a maximum altitude of 134 meters. The parachute was activated at an altitude of approximately 47 meters, and the descent with the parachute took a total of 11 seconds. After the parachute deployment, the UAV descended at a vertical speed of 4.27 m/s, or 14 FPS. The trajectory followed during the flight and the representation of the flight area are depicted in Figure 11. The blue lines represent the UAV flight path.

The altitude-time graph depicting changes in altitude during the UAV flight is presented in Figure 12. The variability in altitude is primarily due to the flight being conducted in stabilized mode with pilot control. Although

autonomous testing could be conducted with GPS support, it was deemed appropriate in this study to conduct flights under pilot control to better control and intervene in UAV responses. In Figure 12, the altitude values obtained from the internal barometric pressure sensor are shown in green, while the altitude change data recorded by the GPS receiver is shown in red. Additionally, the estimated altitude value, derived from the composite of data from GPS and the barometric pressure sensor, is shown in blue. The shaded area in Figure 12 indicates the change in altitude from the activation of the parachute until landing.

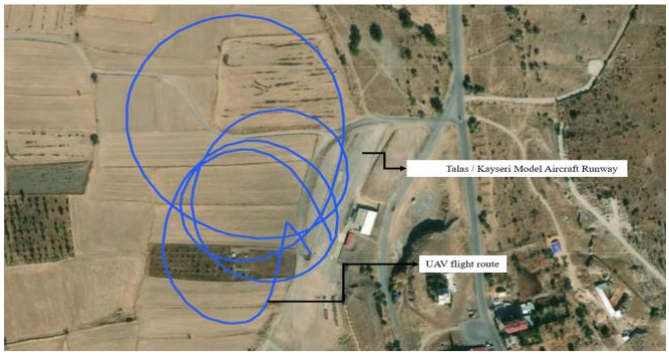


**Figure 11.** UAV Flight Path.

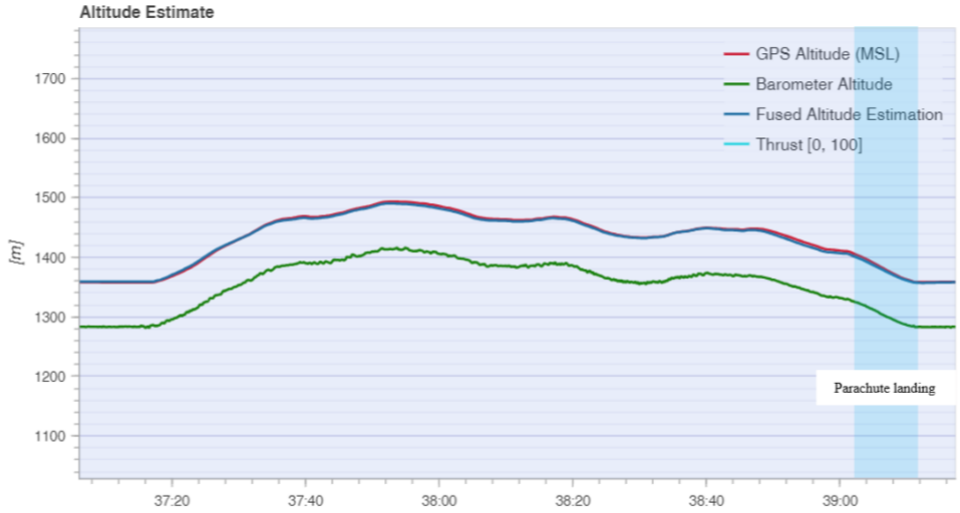


**Figure 12.** UAV Altitude-Time Graph.

Acceleration values over time in the X, Y, and Z axes during the UAV flight are depicted in Figure 13. The blue area in Figure 13 indicates the speed of the UAV after the parachute is deployed. The Z-axis is represented by the blue line, representing the vertical speed of the UAV. The average vertical speed of 4.27 m/s is clearly indicated by the black line.


**Figure 13.** UAV Speed-Time Graph.

When examining parachute systems used worldwide, it is observed that only a few companies manufacture landing and recovery parachutes specifically for UAVs. The reasons for this are both the cost of UAV landing system parachutes and the difficulty of integrating them into UAV systems. Additionally, parachutes designed for mini-UAVs need to occupy minimal volume and have a light mass for the landing system. Consequently, parachute manufacturers tend to avoid producing parachutes with high drag coefficients and low oscillation.

The costs of UAV parachute landing and recovery systems produced by some companies are provided in Table 1. In this study, a low-cost parachute landing system was designed for mini fixed-wing UAVs. The costs of the produced parachute landing system are listed in Table 2. The pricing in Table 2 is calculated based on the quantities of materials used for a parachute system, not on the quantities purchased.

Rescue systems used in unmanned aerial vehicles (UAVs) have shown highly successful results in line with their designated missions. These landing systems are especially critical for UAVs carrying valuable payloads or operating over populated areas. Similarly, rescue systems for manned aircraft have been a subject of research for many years and are considered a significant safety solution in this regard. For

instance, ballistic rescue systems used in popular ultralight aircraft, such as the Cirrus Aircraft SR20 and SR22, have effectively prevented accidents and damage, thereby saving human lives. However, the applicability of similar systems for large passenger aircraft has been limited due to cost and technical challenges. One of the primary factors complicating the integration of these systems is the weight of passenger aircraft. For example, the maximum takeoff weight of one of the most popular aircraft models, the Airbus A320, is 77,000 kg. To safely land an aircraft of this size at a vertical speed of 6-7 m/s, an extremely large parachute would be required, and with current technologies, the production of such a parachute is not feasible. Additionally, considering the critical importance of minimizing weight in commercial aviation, the use of such a large parachute system would present significant cost challenges (Copper, 2024; Airbus, 2024).

**Table 1.** Costs of Various Parachute Landing and Recovery Systems

| Parachute Systems | System Weight | Maximum Usable Weight | Price |
|---|---|---|---|
| Fruity chutes Fixed Wing (1,8 kg) | 221 grams | 1.8 kg | 312$ |
| Fruity chutes Fixed Wing (3,2 kg) | 270 grams | 3.2 kg | 350$ |
| Fruity chutes skycat | 272 grams | 5 kg (2.5 kg optimum weight) | 755,5$ |
| Fruity chutes harrier | 154 grams | 5 kg (2.5 kg optimum weight) | 416.24$ |
| Mars Parachutes (Mars 58) | 277.5 grams | 4.5 kg | 450$ |
| Manufactured Parachute | 465 grams | 2.1 kg | 87$ |

## 4. Conclusion

This study, tested on a UAV with traditional control surfaces, demonstrates that this system can be actively used in many fixed-wing UAVs. The use of ultra-lightweight ripstop fabric and suspension lines in the parachute landing system, along with modern sewing techniques, highlights the original aspects of the study. Additionally, significant cost improvements have been made compared to other parachute systems available in the literature and on the market, thanks to the consumables and production techniques used in the study. Furthermore, the design of the launch system has been conceived considering the opening of the parachute and its integration into different aircraft concepts compared to existing systems. The servo motor used to trigger the launch mechanism, with its low power consumption and high torque, has opened the way for its use in many aircraft. An optimal thrust spring has been used in the launch mechanism to easily activate parachute descent even at low altitudes.

The UAV used in flight tests was controlled by the pilot using the stabilize mode, thanks to the flight control card. After a short take-off and flight phase, the launch mechanism was triggered via a switch previously assigned to the ground control station, and the parachute was released. After 1.42 seconds, the parachute fully opened, and the UAV made a safe landing in the designated area as planned. This descent took 11 seconds, and the vertical speed during descent was recorded as 4.27 m/s (14 FPS), as planned during the design phase. It was determined that the parachute deployment time and the vertical speed of the UAV during descent with the parachute complied with the limits set by aviation authorities and recommended in the literature. It is anticipated that the study will contribute significantly to the widespread use of fixed-wing and civilian UAV systems in the future.

The produced parachute landing system in the study has been proven to be 71% more cost-effective compared to similar systems found in the literature and on the market. Additionally, the parachute weight was determined to be 56 grams without including the launch mechanism. Thus, it has demonstrated a 12% lighter parachute design compared to other systems with similar features. Further studies are aimed at achieving a much lighter design for the launch mechanism in the future. With the advantages achieved in terms of cost and weight in this study, significant contributions are anticipated for the development of landing system designs for fixed-wing UAV systems. This study is expected to contribute to future scientific studies focusing on UAV landing systems.

Common examples of aircraft in which rescue systems are widely used include paragliders, hang gliders, microlights, ultralights, and paramotors. One of the main reasons rescue systems are not utilized in manned aircraft, particularly large passenger planes, is the weight of the mechanisms required to deploy such systems. Even in UAVs, parachute rescue systems require ballistic deployment mechanisms when they exceed certain weight limits. Furthermore, during a free fall, a passenger aircraft, which weighs several tons, would impose significant stress on the parachute lines and fabric, potentially causing damage to the system and leading to failure. For these reasons, while parachute rescue systems offer a viable solution for sport aircraft and ultralight single-engine planes, such systems have yet to be developed for large passenger aircraft.

**Table 2.** Cost of Produced Parachute System

| Material | Model (Type) | Price |
|---|---|---|
| Fabric | 0,66 Oz membrane ripstop | 19$ |
| Length of Shroud Lines | Ripstop nylon lines | 4$ |
| Servo | JX Servo PS-1171MG Metal gear | 10$ |
| Carbon Fibre Tubes | 70mm diameter carbon fibre tube with a wall thickness of 1mm | 12$ |
| Mini Carabiner | Aluminium 5 kN | 5$ |
| Spring | Stainless steel | 5$ |
| Other Expenses | PLA etc. materials | 2$ |
| Parachute Manufacture | Labour | 30$ |
| **Total Price** | | 87$ |

## Conflicts of Interest

There is no conflict of interest regarding the publication of this paper.

## Acknowledgement

This work has been supported by Erciyes University Scientific Research Projects Coordination. The unit is under grant number code FYL-2022-12008.

## References


Abinaya, R., Arravind, R. (2017). Selection of Low-Cost Recovery System for Unmanned Aerial Vehicle. International Research Journal of Engineering and Technology, 4(5), 1074-1078.

Airbus. (2024). A 320 CEO Setting Single-Aisle Standards. https://aircraft.airbus.com/en/aircraft/a320-the-most-successful-aircraft-family-ever/a320ceo (Accessed on September 12, 2024).

Al-Madani, B., Svirskis, M., Narvydas, G., Maskeliūnas, R. and Damaševičius, R. (2018). Design of Fully Automatic Drone Parachute System with Temperature Compensation Mechanism for Civilian and Military Applications. Journal of Advanced Transportation, 2018, ID 2964583, 1-11.

Austin, R. (2010). Unmanned Aircraft Systems – UAVS Design, Development and Deployment. John Wiley &Sons Ltd. New Delhi, India.

Bellis, M. (2019). History of the Parachute (Inventors and Innovations). https://www.thoughtco.com/history-of-the-parachute-1992334 (Accessed on April 20, 2024).

Blom, J.D. (2010). Unmanned Aerial Systems: A Historical Perspective. Combat Studies Institute Press, US Army Combined Arms Center, Fort Leavenworth, Kansas.

Copper, B. (2024). The Plane With A Parachute: A Guide To The Cirrus SR22. https://simpleflying.com/plane-with-parachute-cirrus-sr22-guide/ (Accessed on September 12, 2024).

Federal Aviation Administration. (2015). Parachute Rigger Handbook, Oklahoma City, USA, pp. 1-350.

Gleason, T.J. and Fahlstrom, P.G. (2016). Recovery of UAVs. Encyclopedia of Aerospace Engineering, John Wiley & Sons Ltd.

Historical Review. (2024). https://www.parachutehistory.com/eng/drs.html (Accessed on April 20, 2024).

Kekeç, E. T., Konar, M. and Yıldırım Dalkıran, F. (2020). Realization of Low Cost Useful Variometer Application for Sportive Aviation. Journal of Aviation, 4(1), 79-88.

Kim, H.J., Kim, M., Lim, H., Park, C., Yoon, S., Lee, D., Choi, H., Oh, G., Park, J. and Kim, Y. (2013). Fully Autonomous Vision-Based Net-Recovery Landing System for a Fixed-Wing UAV. IEEE/ASME Transactions on Mechatronics, 18(4), 1320–1333.

Knacke, T.W. (1991). Parachute Recovery Systems Design Manual. Para Publishing, Santa Barbara, California, USA.

Mcwilliams, P. (2023). Different Parachute Types: Styles of Canopy for Skydiving. https://awe365.com/a-summary-of-different-parachute-types/ (Accessed on April 20, 2024).

Oktay, T., Konar, M., Onay, M., Aydın, M. and Mohamed, M.A. (2016). Simultaneous Small UAV and Autopilot System Design. Aircraft Engineering and Aerospace Technology, 88, 818-834.

Parachute. (2024). https://www.newworldencyclopedia.org/entry/Parachute (Accessed on April 20, 2024).

Poynter, D. (1991). The Parachute Manual A Technical Treatise on Aerodynamic Decelerators. 4. Edition. Para Publishing, Santa Barbara, California, USA.

Nakka, R. (2020). Parachute Design and Construction. https://www.nakka-rocketry.net/paracon.html (Accessed on May 5, 2024).

Szafran, K.S. and Kramarski, I. (2019). Fatigue Degradation of the Ram-Air Parachute Canopy Structure. Fatigue of Aircraft Structures, 2019(11), 103–112.

Ultimate Drone Parachute System for All Multicopters, Fixed Wing, UAS. (2024). https://fruitychutes.com/uav_rpv_drone_recovery_parachutes (Accessed on April 19, 2024).

Williams, K.W. (2004). A Summary of Unmanned Aircraft Accident/Incident Data: Human Factors Implications. Federal Aviation Administration, Washington, DC, USA.

Wilson, J. (2024). History of Parachuting and CSPA. https://www.cspa.ca/en/node/228 (Accessed on May 5, 2024).

Wyllie, T. (2001). Parachute Recovery for UAV Systems. Aircraft Engineering and Aerospace Technology, 73(6), 542–551.

Zakaria, M.Y. (2013). Design and Fabrication of Low-Cost Parachute Recovery System for SUAVs. 15th International Conference on Aerospace Sciences & Aviation Technology (ASAT – 15), May 28 - 30, 2013, Cairo, Egypt, 1-15.


**Cite this article:** Yildirim Dalkiran, F., Kirteke, E. (2024). Design and Implementation of A Low-Cost Parachute Landing System for Fixed-Wing Mini Unmanned Aerial Vehicles. Journal of Aviation, 8(3), 198-205.